

## Numerical Modeling of Flow Over Trapezoidal Broad-Crested Weir

Stefan Haun, Nils Reidar B. Olsen & Robert Feurich

To cite this article: Stefan Haun, Nils Reidar B. Olsen & Robert Feurich (2011) Numerical Modeling of Flow Over Trapezoidal Broad-Crested Weir, Engineering Applications of Computational Fluid Mechanics, 5:3, 397-405, DOI: [10.1080/19942060.2011.11015381](https://doi.org/10.1080/19942060.2011.11015381)

To link to this article: <https://doi.org/10.1080/19942060.2011.11015381>



Published online: 19 Nov 2014.



Submit your article to this journal [↗](#)



Article views: 1485



View related articles [↗](#)



Citing articles: 8 View citing articles [↗](#)

## NUMERICAL MODELING OF FLOW OVER TRAPEZOIDAL BROAD-CRESTED WEIR

Stefan Haun\*, Nils Reidar B. Olsen and Robert Feurich

*Department of Hydraulic and Environmental Engineering, The Norwegian University of Science and Technology, S.P. Andersens veg 5, 7491 Trondheim, Norway*

*\* E-Mail: stefan.haun@ntnu.no (Corresponding Author)*

---

**ABSTRACT:** Two computational fluid dynamics (CFD) codes, Flow-3D and SSIIM 2, have been used to calculate the water flow over a trapezoidal broad-crested weir. The two programs apply different algorithms for making the grid and computing the free water surface. Flow-3D uses the Volume of Fluid (VOF) method with a fixed grid, while SSIIM 2 uses an algorithm based on the continuity equation and the Marker-and-Cell method, together with an adaptive grid for the water surface. The results have been compared with measurements from a physical model study, using different discharges. The deviation between the computed and measured upstream water level was between 1.0 and 3.5%. The difference between the results from the two CFD models was in the range of 1–1.5%. The accuracy of the algorithms depends on the grid size. The computational time on one core of a CPU (Intel Q9650 3.00 GHz) was between 435 and 15,500 seconds, using between 6,350 and 10,000 cells.

**Keywords:** numerical models, Volume of Fluid Method, Marker-and-Cell approach, water flow, free water surface

---

### 1. INTRODUCTION

Broad-crested weirs are defined as structures where the streamlines run parallel to each other over the weir crown, and the crest of the weir is horizontal (Bos, 1976). In most layouts of broad-crested weirs also the hydrostatic pressure is fully accomplished in the middle of the crest. However, in cases where the weir length is too small it might be that the hydrostatic pressure is not fully accomplished (Hager, 1986). The broad-crested weir is in addition to irrigation systems used for highways, railroads and for hydropower structures. Also an application as a simple discharge measurement structure is possible. An important feature of a broad-crested weir is the up- and downstream side slope angle, which may vary between a vertical end (standard broad-crested weir) and a 1:2 ramped slope (standard embankment-weir). Sloping embankments have a higher discharge capacity compared to a traditionally broad-crested weir with vertical faces (Fritz and Hager, 1998). The discharge characteristics for vertical face weirs with square-edged or rounded entrance are extensively analysed by Azimi and Rajaratnam (2009).

This paper shows the application of numerical models as a possibility to support designers, by using a simple test study. Unforeseen conditions during construction, like foundation problems or unexpected properties of the construction material,

could demand a new, verified design of the weir (e.g. variation of the side slopes or changes in the length of the crest). Also the necessity for rapid evaluation of new water discharges is an example for the useful application of a numerical model.

First investigations on discharge capacity of broad-crested weirs were made by Bazin in 1898. An extensive series of experiments were conducted by Hager and Schwalt (1994) for evaluating the flow features over a broad-crested weir. Earlier work involving flow modeling over a rectangular broad-crested weir has been conducted by Sarker and Rhodes (2004), who investigated a weir experimentally as well as numerically (the used code was Fluent V.4.4.7). Good agreement was found in the above mentioned case for the upstream water level (stated as excellent), whereas all other numerical results, like rapidly-varied flow profile over the crest, differ slightly from the results of the physical model study. Hargreaves et al (2007) used the Volume of Fluid method (Fluent V.6.2) to compute the discharge also over a vertical faced broad-crested weir. In this work the up- and the downstream water depths in the model were fixed. The main differences between the earlier work and the current publication are the choice of numerical algorithms, the shape of the weir, the number of investigated flow rates and that the water levels are not kept on a fixed up- and downstream value.

In the current paper, two different programs were tested; the commercial program Flow-3D (2010) and the freely available program SSIIM 2 (abbreviation for: a three-dimensional numerical model for Simulation of Sediment movements In water Intakes with Multiblock option) by Olsen (2009). The numerical programs differ mainly through the algorithms for making the grid and computing the free water surface. Results from a physical model test, conducted by Sargison and Percy (2009), are the basis for comparisons and validations in this manuscript. In the present study also results of the velocity field and the pressure distribution are presented to get an overview about the different output possibilities from the different codes. This kind of output provides a good basis for an understanding of the water flow over hydraulic structures.

## 2. NUMERICAL MODELING

A brief introduction of the basic theory for numerical models is given below, including grid types and the calculation of the free water surface.

### 2.1 Basic theory

The continuity (1) and Reynolds-averaged Navier-Stokes (2) equations are for this case solved in a vertical plane (two dimensions), in order to compute the water motion for turbulent flow.

$$\frac{\partial U_i}{\partial x_i} = 0 \quad (1)$$

with  $i = 1, 2$ .

$$\frac{\partial U_i}{\partial t} + U_j \frac{\partial U_i}{\partial x_j} = \frac{1}{\rho} \frac{\partial}{\partial x_j} \left( -P \delta_{ij} + \rho \nu_T \left( \frac{\partial U_i}{\partial x_j} + \frac{\partial U_j}{\partial x_i} \right) \right) \quad (2)$$

where  $U$  is the Reynolds-averaged velocity over time  $t$ ,  $x$  is the spatial geometrical scale,  $\rho$  is the water density,  $P$  is the Reynolds-averaged pressure,  $\delta$  is the Kronecker delta and  $\nu_T$  is the turbulent eddy-viscosity.

Different discretization schemes are used by the CFD codes in this investigation, to transform the partial differential equations into algebraic equations that can be solved within the grid. Flow-3D uses the finite-difference method and a conservative formulation, while SSIIM 2 uses the finite-volume method. The turbulence is predicted by the standard  $k-\varepsilon$  model (turbulent kinetic energy  $k$  and its dissipation  $\varepsilon$ ) using the constant empirical values by Launder and Spalding (1972). The pressure is calculated according to the

SIMPLE method (Semi-Implicit Method for Pressure-Linked Equations, Patankar, 1980). For the boundaries at the bed and the walls, where the water flux is zero, wall laws were used (Schlichting, 1979), Equation 3.

$$\frac{U}{u^*} = \frac{1}{k} \left( \frac{30y}{k_s} \right) \quad (3)$$

where  $U$  is the velocity,  $u^*$  is the shear velocity,  $k$  is the Karman constant (typically the value 0.4 is used),  $y$  is the water depth and  $k_s$  is the boundary roughness.

### 2.2 Computation of the free water surface

The free water surface represents a particular challenge in 2D vertical and also in 3D numerical models. The selected computer programs use different methods. Flow-3D uses the Volume of Fluid Method (VOF) by Hirth and Nicols (1981). This is a two-phase approach where both the water and the air are modelled in the grid. The method is based on the concept that each cell has a fraction of water ( $F$ ), which is 1 when the element is totally filled with water and 0 when the element is filled with air. If the value is between 1 and 0, the element contains the free water surface. Therefore an additional transport equation is added (Equation 4).

$$\frac{\partial F}{\partial t} + u \frac{\partial F}{\partial x} + v \frac{\partial F}{\partial y} = 0 \quad (4)$$

where  $u$  and  $v$  are fluid velocity components in the  $x$  and  $y$  coordinate direction.

The local height of the water surface, the surface slope and the curvature are calculated for the local column and its neighbours (Figure 1). The VOF method requires a fixed grid in Flow-3D. SSIIM 2 uses an adaptive grid, where the upper boundary

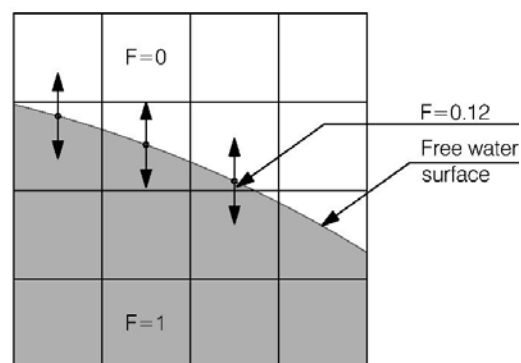


Fig. 1 Assessment of the surface (for a 2D grid) according to the VOF method. The arrows show the potential movement of the water surface.

of the highest grid cell always represents the free water surface. All the cells are thus always completely filled with water. The number of grid cells in the vertical direction depends on the water depth and the initial settings. The vertical movement of the water surface is obtained from the average of the following two methods:

1. The first approach is based on the water continuity in the cell closest to the water surface. The continuity defect over a time step divided by the cell area projected in the horizontal plane gives the vertical water surface movement in the same time step.
2. The second approach is based on a Marker-and-Cell inspired approach. The water surface movement is assumed to follow an imaginary particle in the cell close to the water surface. The average velocity in the surface cell is the same as the particle velocity. Multiplying the vertical water velocity with the time step gives the water surface elevation movement in the time step.

The effective vertical water surface movement,  $\Delta z$ , is thereby given by Equation 5.

$$\Delta z = \frac{1}{2} \left( \frac{\Delta V}{A_2} + \frac{\sum_{n=1}^2 U_n A_n}{A_2} \right) \Delta t \quad (5)$$

where  $U_n$  is the velocity in the surface cell, with component in  $n$  direction.  $A_n$  is the area component on the top of the surface cell, also in direction  $n$ . The horizontal direction is 1, while 2 is the vertical direction.  $\Delta t$  is the time step and  $\Delta V$  is the volume flux deficit in the surface cell. In the current paper, a width-averaged approach is used, so the components in the direction normal to the main flow direction are zero. The formula can also be used for three dimensions.

### 2.3 Grid types

Flow-3D uses a structured and orthogonal grid with rectangular (2D) and hexahedral cells (3D). The non-adaptive grid is fixed and does not move during the calculation. The border between the geometry and the water is defined by the Fractional Area Volume Obstacle Representation (FAVOR) method. Figure 2 shows a longitudinal profile of the grid used in Flow-3D.

SSIIM 2 uses a non-orthogonal, unstructured and adaptive grid with dominantly hexahedral cells (Olsen, 1999). Some tetrahedral cells are allowed in order to reproduce more complex geometries. The main difference compared with other models is that the grid is adaptive. When the water

surface moves, the grid will also move vertically. Hence, only the water phase will be calculated, not the air phase. The grid is regenerated during the computation with a varying number of grid cells over the depth. The number of cells in the vertical direction is a function of the water depth and an empirical value ( $p$ ), Equation 6:

$$n = n_{max} \times \left( \frac{depth}{depth_{max}} \right)^p \quad (6)$$

where  $n$  is the number of grid cells in the vertical direction,  $n_{max}$  is the maximum number of grid cells in the vertical direction,  $p$  is a parameter for number of grid cells (where  $p = 0.5$  gives the best result for this case). Figure 3 shows a longitudinal profile of the grid used by SSIIM 2.

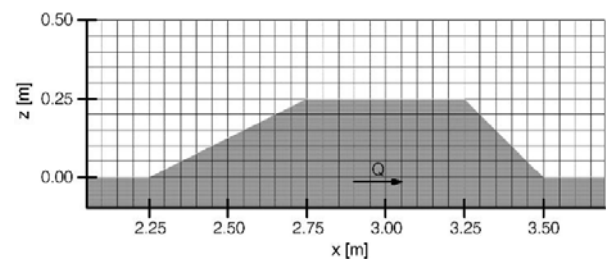


Fig. 2 Sketch of the orthogonal, structured and non-adaptive grid (hexahedral), used in Flow-3D. In the computations a finer grid is used.

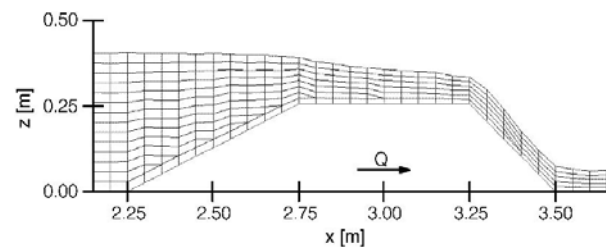


Fig. 3 Sketch of the non-orthogonal, unstructured and adaptive grid (hexahedral and tetrahedral) used in SSIIM 2. In the computations a finer grid is used.

### 2.4 Grid generation

For the calculation with SSIIM 2, the weir configuration was made directly in the program using the implemented grid editor. The weir setup in Flow-3D was performed by inserting an STL (stereolithography) file. In STL files solid object surfaces are approximated by triangles. Most CAD programs are able to convert solid models into an STL format (Flow-3D, 2010). To save computation time, an initial water body in front of the weir was inserted. A grid sensitivity analysis, with respect to the computational time, was made for both programs in the same way. The grid was

refined until the computation time increased disproportionately, compared with the achieved accuracy (mainly in SSIIM 2). This was chosen as criteria, because it is not straightforward to compare different types of grids. The cell size at the beginning was 5 cm in the  $x$ -direction. For the final computations the cell size was decreased to 2 cm in the  $x$ -direction in Flow-3D and to 1 cm in SSIIM 2. In the  $z$ -direction the size of the cells for Flow-3D was chosen equal 2 cm. In SSIIM 2 the number of cells varies during the computation, regarding the adaptive grid. Table 1 shows the result for the upstream water level ( $h_1$ ) for the same discharge and the disproportionately increased computation time in SSIIM 2.

Table 1 Results of grid sensitivity analysis for the upstream water level  $h_1$ .

| Test # | Q [m <sup>3</sup> /s] | cell size (x) [cm] | $h_1$ , Flow-3D [m] | $h_1$ , SSIIM 2 [m] | comp. time, SSIIM 2 [sec] |
|--------|-----------------------|--------------------|---------------------|---------------------|---------------------------|
| 1      | 0.0181                | 5.0                | 0.3929              | 0.3906              | 550                       |
| 2      | 0.0181                | 2.0                | 0.3931              | 0.3912              | 1000                      |
| 3      | 0.0181                | 1.0                | 0.3933              | 0.3925              | 12,500                    |

## 2.5 Time step

A Courant-type stability criterion is used in Flow-3D to calculate the maximum allowed time-step size. The Courant Number tells how fast the fluid passes through a cell. If the Courant Number is greater than 1, the velocity of a particle is so high that it passes through a cell in less than one time step. This leads to numerical instabilities. The stability criteria in Flow-3D lead to time-steps between 0.0016 and 0.0019 seconds. In SSIIM 2 a manually chosen time step is required. The time step for the calculation with SSIIM 2 was chosen with a value of 0.0005 seconds to avoid instabilities in the computations.

## 2.6 Boundary conditions

A constant volume flow rate is used as inflow boundary in Flow-3D and SSIIM 2. In Flow-3D the grid covers the whole flume, so the inflow would be distributed over the whole flume depth. That is not correct, so the area of the inlet above the expected water surface was blocked out to specify the inflow height. Otherwise the inflow would produce waves in the upstream part of the weir, which would influence the results. Through the fixed grid in Flow-3D, an inflow height of 0.35 m for the discharges 0.0181 m<sup>3</sup>/s, 0.0152 m<sup>3</sup>/s, 0.0109 m<sup>3</sup>/s and 0.0079 m<sup>3</sup>/s was chosen and 0.32 m for 0.0055 m<sup>3</sup>/s. Due to the use of adaptive grid in SSIIM 2, the inflow height is computed by the program. The outflow water

depth was chosen manually to be 0.038 m for all discharge values (which is required for the calculation). A zero gradient outflow boundary condition is chosen in SSIIM 2. Flow-3D uses a continuative boundary outflow condition, which consists of zero normal derivatives at the boundary for all quantities, and represents a smooth continuation of the flow through the boundary (Flow-3D, 2010).

All results in this paper are based on a roughness of 2 mm in absence of specified parameters from the physical model. As the roughness is a very important factor in numerical models, a sensitivity analysis was conducted. Calculations for the largest discharge were therefore made for a roughness of 1 mm and 0.1 mm, respectively. The results are shown in Table 2.

Table 2 Results of roughness sensitivity analysis for the upstream water level  $h_1$ .

| Test # | Q [m <sup>3</sup> /s] | roughness [mm] | $h_1$ , Flow-3D [m] | $h_1$ , SSIIM 2 [m] |
|--------|-----------------------|----------------|---------------------|---------------------|
| 1      | 0.0181                | 2.0            | 0.3933              | 0.3925              |
| 2      | 0.0181                | 1.0            | 0.3929              | 0.3918              |
| 3      | 0.0181                | 0.1            | 0.3927              | 0.3910              |

## 2.7 Convergence criteria

The solution in Flow-3D converges if the viscous and the pressure iterations have converged. The convergence criteria are the same for the pressure iteration as for the explicit viscous algorithm. They are set automatically during the calculation and may vary between time steps. In SSIIM 2, the convergence criteria are based on the water continuity, residuals for the Navier-Stokes equations and the turbulence equations of the  $k$ - $\epsilon$  model. The scaled residual should be under 0.001.

## 3. EXPERIMENTAL TESTS

The measurements by Sargison and Percy (2009) were conducted in a horizontal research flume with a width ( $b$ ) of 0.2 m, a height ( $h$ ) of 0.4 m, a total length ( $l$ ) of 5.4 m and a slope angle of 0 degree. The weir configuration ARB from the physical model was chosen in the current study, where A (1:2) is the upstream and B (1:1) the downstream slope. The component R is the rectangular part in between. The notations in this paper are kept identical to those defined by Sargison and Percy (2009). The component dimensions and notations are shown in Figure 4 and Table 3.

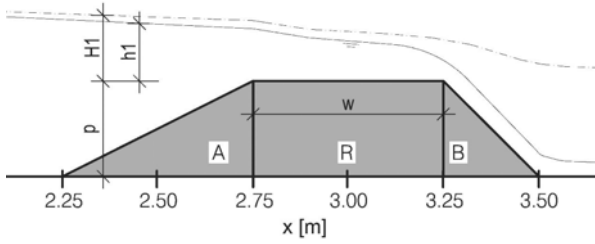


Fig. 4 Longitudinal cross-section of the investigated broad-crested weir. The water flow is from left to the right.

Table 3 Component dimensions used in investigations.

| Flume: |         | Weir: |                   |
|--------|---------|-------|-------------------|
| l      | 5400 mm | p     | 250 mm            |
| b      | 200 mm  | w     | 500 mm            |
| h      | 400 mm  | A     | 2H : 1V           |
| slope  | 0%      | B     | 1H : 1V           |
|        |         | R     | Rectangular crest |

The steady flow rate varied between 0.0181 and 0.0055 m<sup>3</sup>/s. The tail water level was chosen in a way that would not affect the incoming flow. For the headwater, a uniform flow in front of the weir was given. The water surface was measured with an accuracy of ± 0.5 mm using a point gauge on a traverse apparatus and the volumetric flow rate with ± 0.01 l/s using a 90° V-notch weir. The key parameters and the results from the lab tests are shown in Table 4.

Table 4 Key parameters and results from the physical model (ph.m.) test by Sargison and Percy (2009).

| Test # | Q [m <sup>3</sup> /s] | h <sub>1, ph.m.</sub> [m] | H <sub>1, ph.m.</sub> [m] |
|--------|-----------------------|---------------------------|---------------------------|
| 1      | 0.0181                | 0.147                     | 0.150                     |
| 2      | 0.0152                | 0.130                     | 0.133                     |
| 3      | 0.0109                | 0.105                     | 0.106                     |
| 4      | 0.0079                | 0.086                     | 0.087                     |
| 5      | 0.0055                | 0.065                     | 0.066                     |

The chosen setup for the weir results in a free overflow, where the total energy head is given by Equation 7.

$$H_1 = h_1 + [Q^2 / 2gb^2(h_1 + p)^2] \tag{7}$$

where  $H_1$  is the total energy height,  $h_1$  is the water depth,  $Q$  is the flow rate,  $g$  is the acceleration due to gravity,  $b$  is the crest-width and  $p$  is the weir height.

The overflow capacity ( $Q$ ) depends on the discharge coefficient ( $C_d$ ), the crest width ( $b$ ) and the upstream water head ( $H_1$ ), Equation 8.

$$Q = C_d b \sqrt{2gH_1^3} \tag{8}$$

This depth-discharge relationship exists up to a quite high tail-water levels (Woodburn, 1932). According to Fritz and Hager (1998), the discharge coefficient for long broad-crested weirs is nearly constant ( $C_d \approx 0.37$ ). As a limitation, the horizontal length of the weir should not be less than 1.45  $H_{1,max}$  (Bos, 1976).

## 4. RESULTS

Results of the calculated water surface elevation for all five flow rates are given below for Flow-3D and SSIIM 2. Also a comparison of the results with the measurements from the physical model is given, together with a comparison between the results of the two numerical programs.

### 4.1 Flow-3D

The calculation with Flow-3D had a fixed grid with 6,333 active cells. The grid had a cell size of 2 cm in both the  $x$ -direction and the  $z$ -direction. After a computation time in the range of 435–550 seconds, a steady-state solution was found. Also a grid with a smaller cell size (12,539 cells and 1 cm in the  $x$ -direction) was tested, with minor differences in the results, but with an increased computation time (between 750 and 910 seconds), depending on the flow rate. Tests with the RNG turbulence model resulted in negligible differences. The deviation of the upstream water level from the physical model test was between 0.95 and 3.49% for the chosen grid. For the finer grid the deviation did not change.

### 4.2 SSIIM 2

The initial grid (1 cm in the  $x$ -direction) had in total 9,769 cells. The number of grid cells varied through the computation as the grid was adaptive (between 9,311 and 9,460 at the end of the calculation). The computational time of SSIIM 2 depended in this case on the flow rate. After approximately 12,500 seconds for  $Q = 0.0181$  m<sup>3</sup>/s and after 15,500 seconds for  $Q = 0.0055$  m<sup>3</sup>/s, a stable solution for the 2D calculation was found. Tests with a coarser grid (2,320 cells) were also carried out, but the results for the finer grid were significantly better. For the coarser grid, the computation time was just 1,000 seconds for  $Q = 0.0181$  m<sup>3</sup>/s and about 1,800 seconds for  $Q = 0.0055$  m<sup>3</sup>/s.

The deviation of the upstream water level with respect to the physical model test was between 1.54 and 3.49% for the fine grid. A deviation between 3.08 and 5.81% was calculated for the

coarse grid. The grid movement during the computation is shown in Figure 5.

### 4.3 Comparison of numerical results

Longitudinal cross sections including the free water surface profiles for the two CFD programs and three different flow rates are shown in Figures 6–8. All presented values were obtained when the solution had converged.

The results of the two different CFD codes are very similar for all flow rates. The water level ( $h_1$ )

is taken upstream of the weir ( $x = 1.5$  m), where it is approximately constant. The deviation of the upstream water level is in the range of 1–1.5% between the two CFD codes. The discharge coefficients ( $C_d$ ) are calculated using Equation 8 and  $H_1$  is computed from Equation 7. The calculated discharge coefficient varies for the numerical models between 0.355–0.370, depending on the flow rate. The deviations in the discharge coefficient are 0.0–2.2% between Flow-3D and SSIIM 2, where the largest difference was

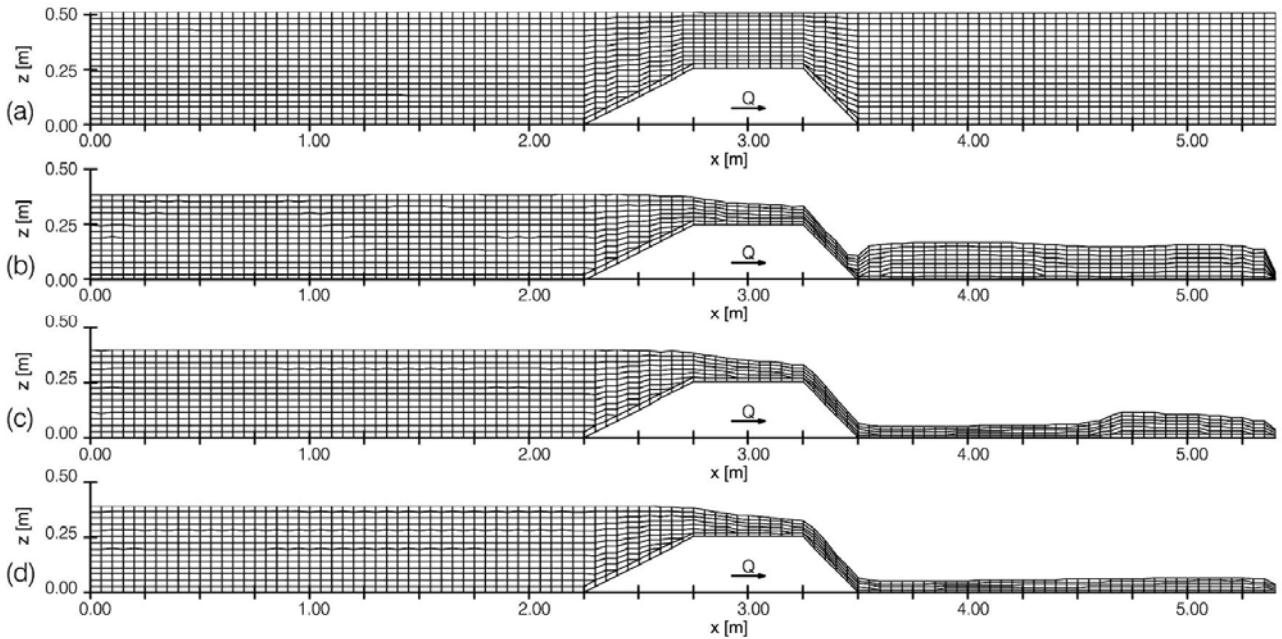


Fig. 5 Free-surface evolution from initial condition (a) to the final free-surface (d) in SSIIM 2. Also the grid after one third (b) and after two third (c) of the computation time is shown. In the computations a finer grid is used.

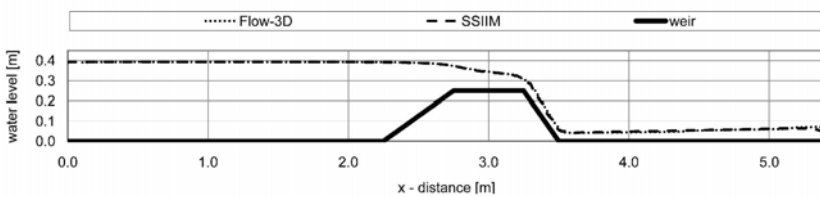


Fig. 6 Longitudinal free-surface profile for  $Q = 0.0181 \text{ m}^3/\text{s}$ .

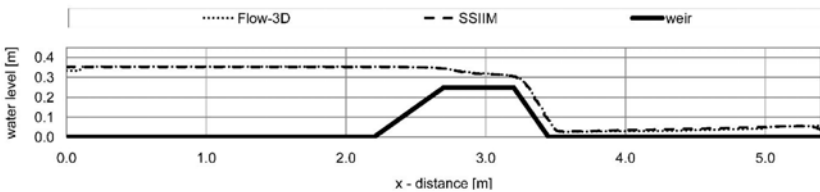


Fig. 7 Longitudinal free-surface profile for  $Q = 0.0109 \text{ m}^3/\text{s}$ .

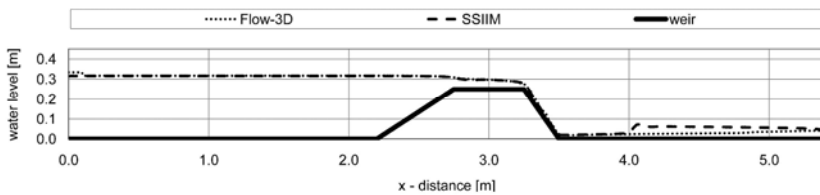


Fig. 8 Longitudinal free-surface profile for  $Q = 0.0055 \text{ m}^3/\text{s}$ .

found for the smallest flow rate. The results of the numerical model tests are shown in Table 5. Figures 9 and 10 show the velocity vectors and the pressure distribution over the weir for the largest discharge, made directly in SSIIM 2. For this kind of structure the hydrostatic pressure is only present at the top of the crown. At the upstream and downstream edge of the crown, the pressure may not be hydrostatic. This is due to significant acceleration of the vertical velocities. For a better understanding of the physics of the flow velocity contour plots are shown in Figure 11. The contour line plot for SSIIM 2 is made in Tecplot 360 and for Flow-3D directly as output of the CFD program.

**5. CONCLUSIONS**

The objective of this study was to evaluate and to validate the flow over a broad-crested weir. The main differences between the two chosen numerical programs are the different free water surface algorithms and the used grid types. A process with successive refinement of an initially coarse grid in order to find grid-independent water levels resulted in the number of required cells for Flow-3D and SSIIM 2 equal to 6,333 and 9,769, respectively. Corresponding computational times are respectively 435–550 and 12,500–15,500 seconds, for the same program order as above. SSIIM 2, with the adaptive grid, needs more cells than Flow-3D to achieve the same accuracy. This is most likely because of the more accurate discretization scheme in Flow-3D. Flow-3D uses a higher order integration to compute the movement of the water surface compared with SSIIM 2. In terms of computation time, the commercial program is significantly more

Table 5 Results from numerical models.

| Test #   | Q [m <sup>3</sup> /s] | h <sub>1, numerical</sub> [m] | $\frac{h_{1,num} - h_{1,ph.n.}}{h_{1,ph.n.}}$ [%] | H <sub>1, numerical</sub> [m] | C <sub>d, num</sub> [-] | $\frac{C_{d,num} - C_{d,ph.n.}}{C_{d,ph.n.}}$ [%] |
|----------|-----------------------|-------------------------------|---|-------------------------------|-------------------------|---|
| Flow 3-D |                       |                               |   |                               |                         |   |
| 1        | 0.0181                | 0.143                         | -2.72   | 0.146                         | 0.367                   | 4.07  |
| 2        | 0.0152                | 0.128                         | -1.54   | 0.130                         | 0.366                   | 2.75  |
| 3        | 0.0109                | 0.104                         | -0.95   | 0.105                         | 0.361                   | 1.57  |
| 4        | 0.0079                | 0.083                         | -3.49   | 0.084                         | 0.368                   | 4.59  |
| 5        | 0.0055                | 0.067                         | 3.08  | 0.067                         | 0.355                   | -3.02   |
| SSIIM 2  |                       |                               |   |                               |                         |   |
| 1        | 0.0181                | 0.143                         | -2.72   | 0.146                         | 0.367                   | 4.07  |
| 2        | 0.0152                | 0.127                         | -2.31   | 0.129                         | 0.370                   | 3.94  |
| 3        | 0.0109                | 0.103                         | -1.90   | 0.104                         | 0.366                   | 3.02  |
| 4        | 0.0079                | 0.083                         | -3.49   | 0.084                         | 0.368                   | 4.59  |
| 5        | 0.0055                | 0.066                         | 1.54  | 0.066                         | 0.363                   | -0.83   |

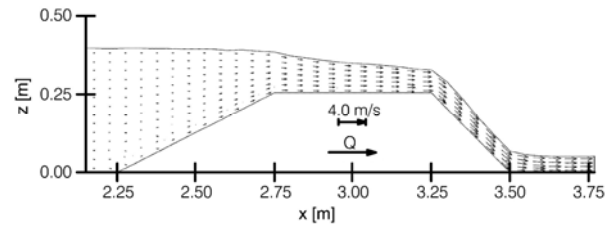


Fig. 9 Velocity vectors for Q = 0.0181 m<sup>3</sup>/s in the area of the broad-crested weir.

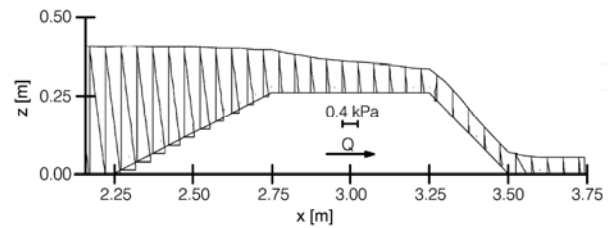


Fig. 10 Pressure distribution for Q = 0.0181 m<sup>3</sup>/s over the weir.

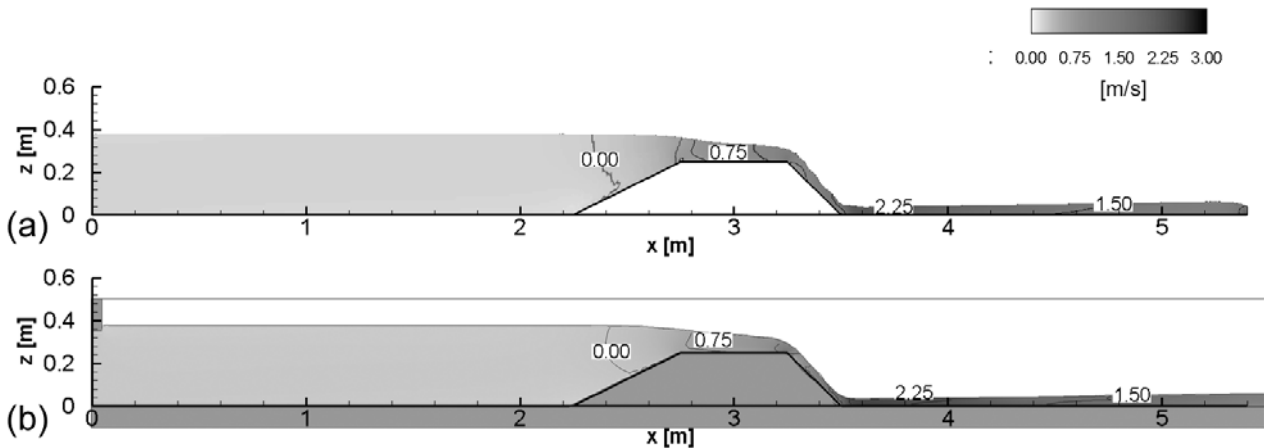


Fig. 11 Velocity contour plots for Q = 0.0152 m<sup>3</sup>/s.

efficient, so the total computation time is much shorter than with SSIIM 2. All computations were made in 2D. 3D tests using Flow-3D gave no differences in the results which agree with the findings of Hargreaves et al. (2007). The time steps highly influence the stability and the computational time. Flow-3D calculates the time step automatically (in the range of 0.0016–0.0019 seconds in this case), whereas the time step was set constant to 0.0005 seconds in SSIIM 2. All runs were made on a personal desktop with one core of a CPU (Intel Q9650 3.00 GHz). However, both codes are parallelized, so simulations with more than one core are possible. This will for example increase the speed by a factor 3 on a quad-core processor. The boundary conditions were set up comparably for both models, but with minor differences due to the differences in the codes.

The two tested numerical models, Flow-3D and SSIIM 2, were both able to predict the water surface profile for the broad-crested weir and the directly linked discharge coefficient. The results from both CFD programs are similar to the results from the physical model test provided by Sargison and Percy (2009). The deviation between the programs seems to be in the same order of magnitude as compared to the physical model. The calculated discharge coefficients for the investigated broad-crested weir are, as stated by Fritz and Hager (1998), nearly constant and equal to 0.37. The computed  $C_d$  is hence considered to be an accurate estimate for the easily applicable discharge coefficient. However, one of the advantages of using a numerical model includes obtaining several flow parameters, like the velocity pattern and the pressure field over the whole area at the same time.

## 6. APPLICATION AND PERSPECTIVE

With the applied free water surface algorithm in SSIIM 2, the results show very small differences compared to the results from Flow-3D. All the numerical simulations were relatively not too time consuming and can therefore, due to the increased computation power, easily be run on a desktop PC. The computational time was between 500 and 15,000 seconds for the models, where Flow-3D required less time than SSIIM 2. However, reliable results require knowledge of the CFD code and numerical modeling in general. Also a good understanding of the problem to be addressed, evaluation of the boundary conditions and high-quality input data are necessary (Olsen, 2010).

Through the development of CFD codes the number of investigated cases increases considerably. The advantage of changing model parameters very fast, like flow rates, the roughness or the size and shape of the weir, is an important factor. A simple weir geometry is used in this case to show the application of commercial software and a free available program. The results show that CFD can be used to compute weir cases, where no discharge coefficients can be found in the literature. Through the use of a numerical program it is also possible to find the flow characteristics for a flow over a weir (e.g. the pressure distribution (over the weir)). The aim should be to develop and use this numerical software in the future for more complex structures, where also 3D effects have to be taken into account in the CFD code. Also an application in different environments is possible for numerical programs. An example for such an environment would be the application to a natural river, where in addition to the water-air interaction, the suspended sediments are a matter of consequences (Bhuiyan and Hey, 2007).

## ACKNOWLEDGEMENTS

The first and the third author are funded by The Research Council of Norway, through the RENERGI programme.

## NOMENCLATURE

|          |   |
|----------|---|
| A        | area [m <sup>2</sup> ]                          |
| b        | weir width transverse to flow direction [m]     |
| $C_d$    | discharge coefficient [-]                       |
| F        | fraction of water [-]                           |
| g        | acceleration due to gravity [m/s <sup>2</sup> ] |
| h        | flume height [m]                                |
| $h_1$    | water depth [m]                                 |
| $H_1$    | upstream overflow total energy head [m]         |
| $k_s$    | boundary roughness [m]                          |
| l        | length of the flume [m]                         |
| p        | weir height [m]                                 |
| Q        | flow rate [m <sup>3</sup> /s]                   |
| U        | water velocity [m/s]                            |
| $u^*$    | shear velocity [m/s]                            |
| w        | length of weir crest [m]                        |
| y        | water depth [m]                                 |
| $\delta$ | Kronecker delta [-]                             |
| $\nu_T$  | turbulent eddy viscosity [m <sup>2</sup> /s]    |
| $\rho$   | water density [kg/m <sup>3</sup> ]              |

## REFERENCES

1. Azimi AH, Rajaratnam N (2009). Discharge characteristics of weirs of finite crest length. *Journal of Hydraulic Engineering* 135(12):1081–1085.
2. Bazin H (1898). Expériences nouvelles sur l'écoulement en d'éversoir. *Annales des Ponts et Chaussées* 68(2):151-265.
3. Bos MG (1976). Discharge measurement structures. *Laboratorium voor Hydraulica an Afvoerhydrologie*, Landbouwhogeschool, Wageningen, The Netherlands, Rapport 4.
4. Bhuiyan F, Hey R (2007). Computation of three-dimensional flow field created by weir-type structures. *Engineering Applications of Computational Fluid Mechanics* 1(4):350–360.
5. Flow-3D (2010). *User Manual Version 9.4*. Flow Science Ink., Santa Fe.
6. Fritz HM, Hager WH (1998). Hydraulics of embankment weirs. *Journal of Hydraulic Research* 124(9):963–971.
7. Hager WH (1986). Discharge measurement structures. *Communication 1*, Chaire de constructions hydrauliques, Département de Génie Civil, EPFL, Lausanne.
8. Hager WH, Schwalt M (1994). Broad Crested Weir. *Journal of Irrigation and Drainage Engineering* 120(1):13–26.
9. Hargreaves DM, Morvan HP, Wright NG (2007). Validation of the volume of fluid method for free surface calculation: the broad-crested weir. *Engineering Applications of Computational Fluid Mechanics* 1(2):136–147.
10. Hirt CW, Nichols BD (1981). Volume of fluid (VOF) method for the dynamics of free boundaries. *Journal of Computational Physics* 39:201–225.
11. Launder BE, Spalding DB (1972). *Lectures in mathematical models of turbulence*. Academic Press, London.
12. Olsen NRB (1999). *Computational Fluid Dynamics in Hydraulic and Sedimentation Engineering*. Class Notes, Department of Hydraulic and Environmental Engineering, The Norwegian University of Science and Technology.
13. Olsen NRB (2009). *A three-dimensional numerical model for simulation of sediment movements in water intakes with multiblock option*. User's Manual, by Nils Reidar B. Olsen, Department of Hydraulic and Environmental Engineering, The Norwegian University of Science and Technology.
14. Olsen NRB (2010). *Result assessment methods for 3D CFD models in sediment transport computations*. 1st Conference of the European section of the IAHR, Edinburgh, Scotland.
15. Patankar SV (1980). *Numerical Heat Transfer and Fluid Flow*. McGraw-Hill Book Company, New York.
16. Sargison JE, Percy A (2009). Hydraulics of Broad-Crested Weirs with Varying Side Slopes. *Journal of Irrigation and Drainage Engineering* 135(1):115-118.
17. Sarker MA, Rhodes DG (2004). Calculation of free-surface profile over a rectangular broad-crested weir. *Flow Measurement and Instrumentation* 15:215-219.
18. Schlichting H (1979). *Boundary layer theory*. McGraw-Hill Book Company, New York.
19. Williams JJR (2007). Free-surface simulations using an interface-tracking finite-volume method with 3D mesh movement. *Engineering Applications of Computational Fluid Mechanics* 1(1):49–56.
20. Woodburn JG (1932). Tests on broad crested weirs, *Trans. ASCE* 1797 96:387–408.